Princeton Plasma Physics Laboratory

PPPL-4175

PPPL-4175

Electron Bernstein Wave Research on Overdense Plasmas in the National Spherical Torus Experiment

G. Taylor, T.S. Bigelow, J.B. Caughman, M.D. Carter, S. Diem, P.C. Efthimion, R.A. Ellis, N.M. Ershov, E. Fredd, R.W. Harvey, J. Hosea, J. Jaeger, B. LeBlanc, C.K. Phillips, J. Preinhaelter, A.K. Ram, D.A. Rasmussen, A.P. Smirnov, J. Urban, J.B. Wilgen, and J.R. Wilson

June 2006

PPPL PRINCETON PLASMA PHYSICS LABORATORY

Prepared for the U.S. Department of Energy under Contract DE-AC02-76CH03073.

Princeton Plasma Physics Laboratory
Report Disclaimers

Full Legal Disclaimer

Trademark Disclaimer

PPPL Report Availability

Princeton Plasma Physics Laboratory

This report is posted on the U.S. Department of Energy's Princeton Plasma Physics Laboratory Publications and Reports web site in Fiscal Year 2006.

The home page for PPPL Reports and Publications is:

http://www.pppl.gov/pub_report/

Office of Scientific and Technical Information (OSTI):

Available electronically at: http://www.osti.gov/bridge.

Available for a processing fee to U.S. Department of Energy and its contractors, in paper from:

U.S. Department of Energy
Office of Scientific and Technical Information
P.O. Box 62
Oak Ridge, TN 37831-0062

Telephone: (865) 576-8401

Fax: (865) 576-5728

E-mail: reports@adonis.osti.gov

Electron Bernstein Wave Research on Overdense Plasmas in the National Spherical Torus Experiment

G. Taylor[1], T.S. Bigelow[2], J.B. Caughman[2], M.D. Carter[2], S. Diem[1], P.C. Efthimion[1], R.A. Ellis[1], N.M. Ershov[3], E. Fredd[1], R.W. Harvey[4], J. Hosea[1], F. Jaeger[2], B. LeBlanc[1], C.K. Phillips[1], J. Preinhaelter[5], A.K. Ram[6], D.A. Rasmussen[2], A.P. Smirnov[3], J. Urban[5], J.B. Wilgen[2], J.R. Wilson[1]

[1]*Plasma Physics Laboratory, Princeton University, Princeton, NJ 08543, USA*
[2]*Oak Ridge National Laboratory, Oak Ridge, TN 37831, USA*
[3]*Moscow State University, Moscow, Russia*
[4]*CompX, Del Mar, CA 92014, USA*
[5]*Czech Institute of Plasma Physics, Prague, Czech Republic*
[6]*Plasma Science and Fusion Center, MIT, Cambridge, MA 02139, USA*

Abstract. Off-axis radiofrequency-driven current is expected to be critical for stabilizing and sustaining solenoid-free spherical torus (ST) plasmas when $\beta > 20\%$. Electron Bernstein wave current drive (EBWCD) may be able to generate the required off-axis current in the overdense ($\omega_{pe} >> \omega_{ce}$) ST plasma regime. Fokker-Planck and 3-D EBW ray-tracing models and EBW emission (EBE) measurements are being used to study EBW coupling, propagation, damping and EBWCD physics in NSTX. This research supports the proposed implementation of a multi-megawatt EBWCD system on NSTX that utilizes EBW coupling via obliquely launched, elliptically polarized, electromagnetic waves and efficient off-axis current generation via Ohkawa EBWCD. EBWCD modeling for plasmas with β of 20-40% and launch frequencies between 14 and 28 GHz predicts current drive efficiencies of 30-50 kA/MW and EBW-driven current densities that peak well off-axis on the outboard side of the NSTX plasma. The thermal EBE coupling efficiency has been measured to be 80±20% at 16-18 GHz, with the coupling efficiency and emission polarization being in good agreement with modeling. The NSTX EBE diagnostic has recently been upgraded to include two remotely steered, quad-ridged antennas, capable of detecting EBE at 8-18 and 18-40 GHz.

Email: gtaylor@pppl.gov

INTRODUCTION

Magnetically confined spherical torus (ST) plasmas, such as those in the National Spherical Torus Experiment (NSTX) [1], offer an attractive design path for a high β fusion reactor only if the plasma can be sustained non-inductively. Off-axis radiofrequency-driven current is expected to be critical for stabilizing solenoid-free ST plasmas when $\beta > 20\%$ [2]. Since ST plasmas are inherently overdense ($\omega_{pe} >> \omega_{ce}$) conventional ECCD cannot provide this off-axis current. Electron Bernstein wave

current drive (EBWCD) has the potential to generate this stabilizing off-axis current in the overdense ST plasma regime. Fokker-Planck and 3-D EBW ray-tracing models and EBW emission diagnostics (EBE) are being employed to study EBW coupling, propagation, damping and EBWCD physics to guide the design of a multi-megawatt EBWCD system planned for NSTX. The EBWCD system design includes ~100% EBW coupling via obliquely launched, elliptically polarized, electromagnetic waves [3,4] and efficient off-axis EBWCD via Ohkawa [5] current drive in a region of the NSTX plasma dominated by magnetically-trapped electrons [6]. This paper summarizes recent modeling results for EBWCD, and EBE coupling measurements and modeling on NSTX.

EBWCD MODELING RESULTS

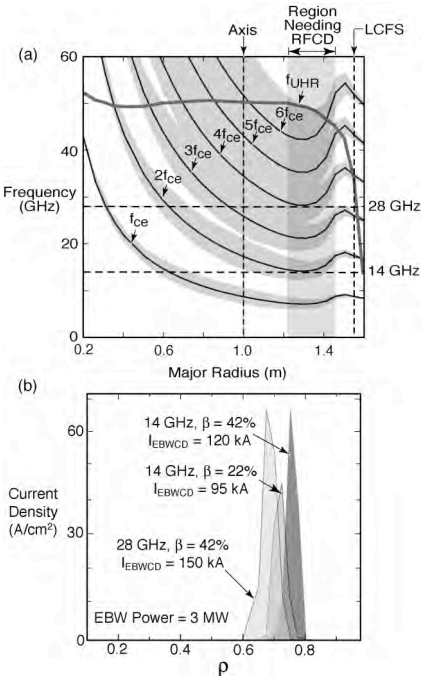

FIGURE 1. (a) Characteristic frequency plot for β = 42% NSTX plasma. The plasma is overdense up to $6f_{ce}$. Shaded regions represent $N_{//} = \pm 1$ Doppler broadening of electron cyclotron resonances. Coupling to EBWs occurs near the UHR frequency (f_{UHR}). (b) Current density profile, calculated by CQL3D, plotted versus normalized minor radius, generated by 3 MW of EBW power at 14 GHz and 28 GHz for NSTX β = 22% and 42% plasmas. The vacuum toroidal field on axis is 0.35T.

The GENRAY numerical ray tracing code [7,8] and the CQL3D Fokker-Planck code [9] have modeled EBW propagation and damping and EBWCD in NSTX plasmas with β > 20% [6]. Figure 1(a) shows the characteristic electron resonance frequencies versus major radius (R) on the midplane of a β = 42% NSTX plasma. Mode conversion between EBWs and electromagnetic waves occurs at the upper hybrid resonance (UHR) that surrounds the overdense plasma. A magnetic field well near the core depresses the electron cyclotron frequency (f_{ce}) outboard of the magnetic axis. EBWs propagating in from the UHR typically experience a significant Doppler shift so that $N_{//}$ (=$ck_{//}/\omega$) ~ 1. As a result, EBWs are strongly damped well before they reach the non-Doppler shifted electron cyclotron resonances shown in Fig.1(a). In Fig. 1(a) the shaded regions represent $N_{//} = \pm 1$ Doppler broadening of each electron cyclotron resonance. The Doppler broadening combined with the magnetic field well limits accessibility for EBWCD to the outer regions of β > 20% NSTX plasmas when the EBW launch frequency is above $2f_{ce}$ at the UHR. In order to non-inductively sustain this β = 42% plasma, ~100kA of RFCD is needed in the region between R = 1.2 m and R= 1.45 m, or at a normalized minor radius (ρ) between 0.4 and 0.8 [2]. Figure 1 (b) shows CQL3D results for the EBW-driven current density versus ρ for 3 MW of 14 and 28 GHz EBW power launched

into a $\beta = 22\%$ and 42% NSTX target plasma. The EBW-driven current density peaks between $\rho = 0.6$ and 0.8 and the total EBW-driven current is ~ 100 kA. The normalized EBWCD efficiency, ζ_{ec} [10], is in the range 0.6 to 0.75, about twice the value of ζ_{ec} measured for ECCD near the axis of a large aspect ratio, conventional Tokamak [11]. The synergy between the EBWCD and the current driven by the electron bootstrap effect has been calculated to be relatively weak, typically <10%. However, locally bootstrap current density increases in proportion to increased plasma pressure, and this effect can significantly affect the radial profile of the rf-driven current density [12].

Figure 2(a) shows a velocity space plot of the strength of the rf-driven quasilinear velocity space diffusion coefficient (contours) and the electron flux due to rf-driven diffusion (arrows) plotted at the peak the EBW-driven current density for the case with 28 GHz EBWCD in Fig. 1. The length of the arrows indicates the logarithm of the magnitude of the electron flux. Figure 2(b) shows a plot of the total electron flux, due to both Coulomb collisions and rf diffusion. Here the length of the arrows indicates the linear magnitude of the electron flux. The rf-diffusion coefficient, due to EBWs damping on the Doppler-downshifted fourth electron cyclotron harmonic resonance, peaks near the trapped-passing boundary. There is a strong electron flux from the population of transiting electrons having negative parallel velocity across the trapped-passing boundary and as a result a negative Ohkawa [5] current is generated. Consequently efficient off-axis current drive is expected in NSTX even in regions of the plasma with a large fraction of trapped electrons [6].

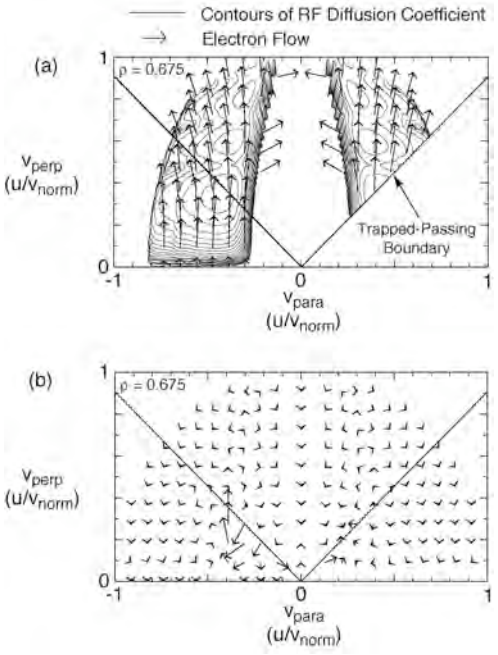

FIGURE 2. (a) Contours of the rf-driven diffusion coefficient calculated with CQL3D plotted in velocity space at the peak of the EBW generated current profile for the case with 28 GHz EBWCD in a $\beta = 42\%$ NSTX plasma shown in Fig. 1. Arrows show electron flux due to the rf diffusion (logarithmic length of flux vector). (b) Total electron flux due to Coulomb collisions and rf diffusion plotted in velocity space (linear length of flux vector). Velocities are normalized to v_{norm}, the momentum per rest mass corresponding to an electron normalization energy = 25 keV.

EBW COUPLING MEASUREMENTS AND MODELING

Electromagnetic radiation can couple to EBWs either at normal incidence to the magnetic field when launched with extraordinary mode polarization (X-B coupling) [13] or at oblique incidence to magnetic field when launched with ordinary mode polarization (O-X-B conversion) [3]. EBW coupling physics is reversible [14], except

for nonlinear effects, such as parametric decay instabilities, so studying mode-converted thermal EBE with absolutely calibrated radiometers provides experimental benchmarking of numerical simulations of EBW coupling. The advantage of X-B coupling is that it is always normal to the field and so it is not necessary to steer the antenna. The disadvantage of X-B coupling is that it is very sensitive to changes in the density scale length (L_n) at the UHR. On the CDX-U ST, ~100% B-X coupling was achieved using a limiter to establish the optimum L_n for B-X coupling at the UHR (~ 7 mm) [15]. NSTX has a higher edge magnetic field than CDX-U, so the optimum L_n is much shorter, typically ~ 3 mm. B-X emission experiments on NSTX achieved only L_n ~ 7 mm and a maximum measured coupling efficiency ~ 40% [16].

Initial B-X-O coupling studies on NSTX where performed with a dual-channel, 8-18 GHz radiometer connected to a fixed, obliquely-viewing, quad-ridged antenna with its ridges aligned to simultaneously measure the radiation temperature of EBE polarized parallel ($T_{//}$) and perpendicular ($T_{\perp}$) to the magnetic field at the UHR [17]. The antenna was aligned for maximum B-X-O coupling efficiency at 16-18 GHz when the magnetic field pitch at the UHR was 35-40 degrees. An example of data from this antenna is shown in Fig. 3(a), which shows the evolution of the EBE radiation temperature, T_{rad} ($=T_{//}+T_{\perp}$) for a L-mode plasma with a vacuum axial toroidal magnetic field of 4 kG and a flattop current of 800 kA between 0.27 and 0.46 s. The EBW coupling efficiency, $(T_{//}+T_{\perp})/T_e$, where T_e is the electron temperature of the EBW emitting layer, was measured to be 80 ± 20% at 16.5 GHz (Fig. 3a). This coupling efficiency was in good agreement with the ~ 65% EBW coupling efficiency predicted by a model that includes a 1-D full wave calculation of the EBW mode conversion at the UHR, radiometer antenna pattern modeling and 3-D EBW ray tracing and deposition modeling [18]. The measured EBE polarization ratio, $T_{//}/T_{\perp}$, was measured to be 1.2, slightly lower than the ratio of 1.5 predicted by modeling (Fig. 3(b)). Emission at 16.5 GHz was from the fundamental electron cyclotron resonance at the plasma magnetic axis during the plasma current flattop

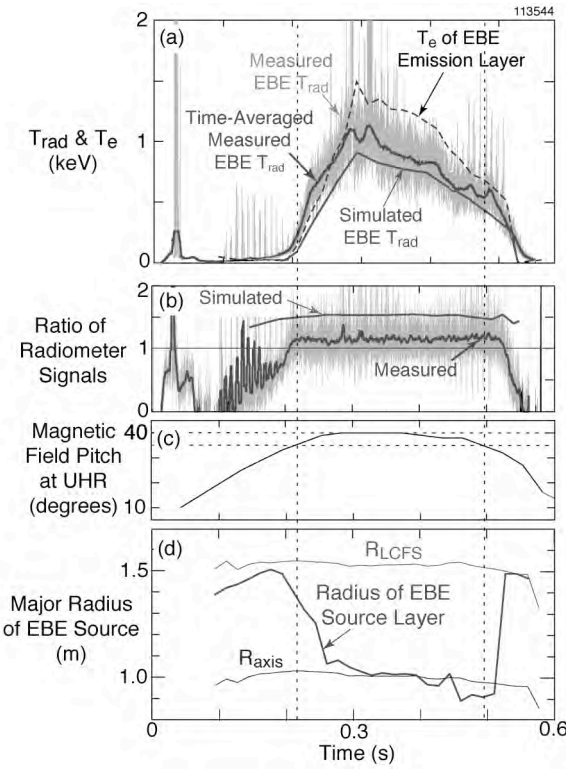

FIGURE 3. (a) The evolution of the measured EBE $T_{//}+T_{\perp}$ signal and the calculated $T_{//}+T_{\perp}$. The ratio of measured $T_{//}+T_{\perp}$ to T_e at the emission layer was 80±20% (dashed line). (b) The EBE polarization ratio, $T_{//}/T_{\perp}$, measured by the dual-channel radiometer compared to the modeled ratio. (c) Variation of the magnetic field pitch at the UHR, the antenna was aligned to measure efficient EBE coupling when the pitch was 35-40 degrees. (d) Modeled radius of the EBE source layer.

(Fig. 3(d)). Rapid fluctuations were observed in both ($T_{//}+T_{\perp}$) and $T_{//}/T_{\perp}$, possibly resulting from L_n fluctuations near the UHR.

Last year, an 18-40 GHz quad-ridged antenna, with limited local steering in the poloidal and toroidal direction, was installed on NSTX. A comparison of measured and simulated EBE data acquired with this diagnostic is shown in Fig. 4(a). T_e measured by Thomson scattering near the UHR in this case was only ~ 15 eV. EBW collisional damping at the UHR may be significant at this T_e. The measured EBE T_{rad} evolution at 25 GHz (solid line) is much lower than the simulated T_{rad} assuming no EBW collisional loss at the UHR (long dashed line). Including EBW collisional loss in the simulation (short dashed line) reduces the simulated T_{rad}, by about 50%, but not enough to match the measured EBE T_{rad}. Figure 4(b) shows a characteristic frequency plot versus major radius at the midplane. Doppler broadening of the electron cyclotron layer for $N_{//} = \pm 1$ is indicated by the shading. EBE simulation results predict that 25 GHz EBE measured by the antenna was radiated predominantly well off-axis from the Doppler-downshifted $3f_{ce}$ resonance. The large fluctuations in simulated EBE T_{rad} evident in Fig. 4(a) for the case with EBW collisional damping at the UHR are due to small changes in T_e at the UHR. There are only a few T_e data points available from laser Thomson scattering in the vicinity of the UHR and there is a steep T_e gradient in this region, so there are significant uncertainties in what T_e actually is at the UHR. Clearly EBW collisional damping may present a significant challenge for a viable EBWCD system if T_e cannot be maintained above ~ 30 eV at the UHR. However, it is possible that the significant radiofrequency power densities present in front of a megawatt-level EBWCD antenna will be sufficient to heat the plasma in the vicinity of the UHR so that T_e is maintained well above 30 eV.

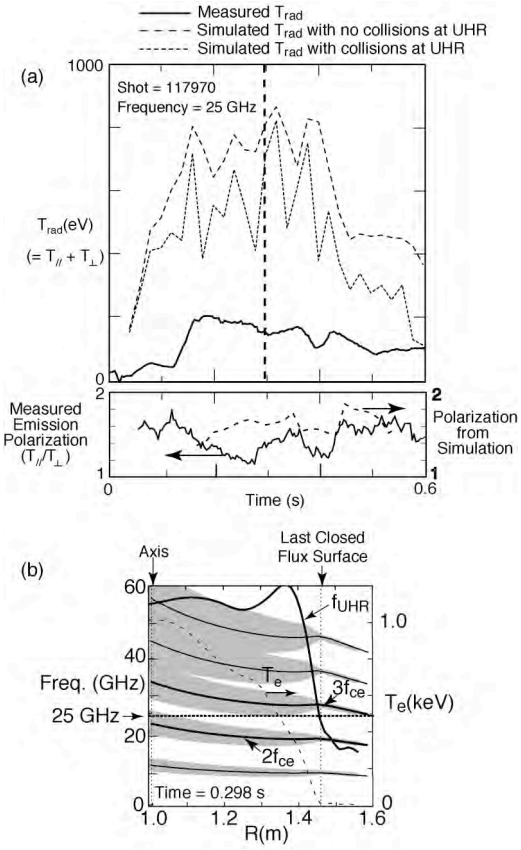

FIGURE 4. (a) Time evolution of the measured EBE T_{rad} at 25 GHz (solid line), compared to the simulated T_{rad} with no EBW collisional loss at the UHR (long dashed line), and with collisional loss at the UHR (short dash) for NSTX shot 117970. Measured EBE polarization ($T_{//}/T_{\perp}$) agrees well with the EBE simulation. (b) Characteristic electron frequencies and electron temperature profile versus major radius plotted at 298 ms for shot 117970. Shading indicates $N_{//} = \pm 1$ Doppler broadening.

Recently, two remotely steered quad-ridged antennas, covering 8-18 and 18-40 GHz became operational on NSTX [19]. The antennas can be steered between shots to

map the EBW mode conversion efficiency versus toroidal and poloidal angle. Each

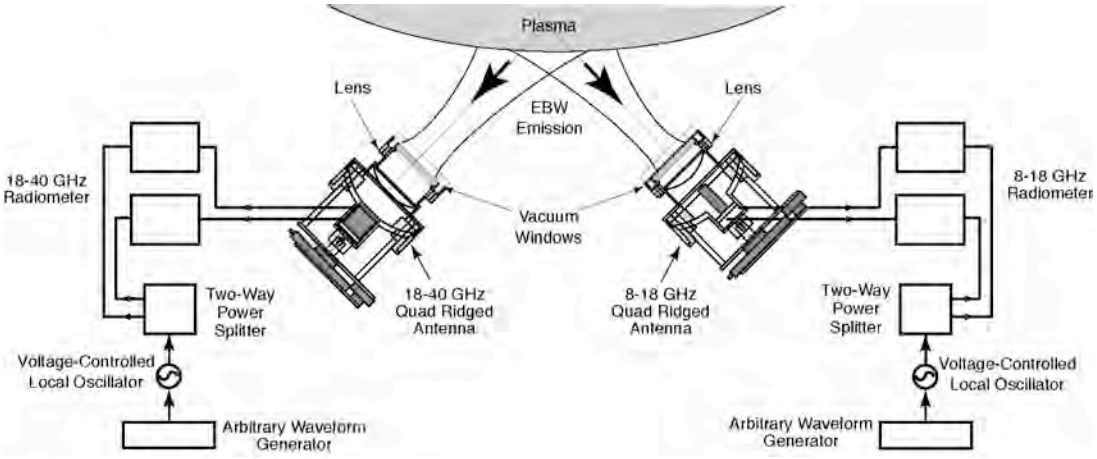

FIGURE 5. Schematic layout of dual channel 8-18 GHz and 18-40 GHz EBE radiometers on NSTX.

antenna can be steered at least $\pm 10^{o}$ in the poloidal and toroidal. Initial EBE measurements from these new antennas are being analyzed.

ACKNOWLEDGMENTS

This research was supported by United States Department of Energy contracts DE-AC02-76CH03073, DE-FG02-91ER-54109, DE-FG03-02ER54684, DE-FG02-99ER-54521 and a grant to encourage innovations in fusion diagnostic systems.

REFERENCES

1. M. Ono, *et al.*, Nucl. Fusion **40**, 557 (2000).
2. C.E. Kessel, *et al.*, Nucl. Fusion **45**, 814 (2005).
3. J. Preinhaelter, and V. Kopécky, J. Plasma Phys. **10**, 1-12 (1973).
4. H. Igami, *et al.*, Plasma Phys. Controlled Fusion **46**, 261 (2004).
5. T. Ohkawa, "*Steady state operation of tokamaks by RF heating*", GA Report GA-A13847 (1976). See National Technical Information Document No.PB2000-108008.
6. G. Taylor, *et al.*, Phys. Plasmas **11**, 4733 (2004).
7. A.P. Smirnov, and R.W. Harvey, Bull. Am. Phys. Soc. **40**, 1837 (1995).
8. C.B. Forest, *et al.*, Phys. Plasmas **7**, 1352 (2000).
9. R.W. Harvey, and M.G. McCoy, *Proceedings of the IAEA Technical Committee on Advances in Simulation and Modeling of Thermonuclear Plasmas*, Montreal, Quebec (International Atomic Energy Agency, Vienna, 1993), p. 489; USDOC NTIS Doc. No. DE93002962.
10. T.C. Luce, *et al.*, Phys. Rev. Lett. **83**, 4450 (1999).
11. C.C. Petty, *et al.*, Nucl. Fusion **42**, 1366 (2002).
12. R.W. Harvey and G. Taylor, Phys. Plasmas **12**, 051509 (2005).
13. A.K. Ram, and S.D. Schultz, Phys. Plasmas **7**, 4084 (2000).
14. A. Bers and A.K. Ram, Physics Letters **301**, 442 (2002).
15. B. Jones, *et al.*, Phys. Rev. Lett. **90**, 165001 (2003).
16. G. Taylor, *et al.*, Phys. Plasmas **10**, 1395 (2003).
17. G. Taylor, *et al.*, Phys. Plasmas **12**, 052511 (2005).
18. J. Preinhaelter, *et al.*, p. 349 AIP Conf. Proc. **787**, 349 (2005).
19. S. Diem, *et al*, *"$T_e(R,t)$ Measurements using Electron Bernstein Wave Thermal Emission on NSTX"* submitted to Rev. Sci. Instrum. (2006).

External Distribution

Plasma Research Laboratory, Australian National University, Australia
Professor I.R. Jones, Flinders University, Australia
Professor João Canalle, Instituto de Fisica DEQ/IF - UERJ, Brazil
Mr. Gerson O. Ludwig, Instituto Nacional de Pesquisas, Brazil
Dr. P.H. Sakanaka, Instituto Fisica, Brazil
The Librarian, Culham Science Center, England
Mrs. S.A. Hutchinson, JET Library, England
Professor M.N. Bussac, Ecole Polytechnique, France
Librarian, Max-Planck-Institut für Plasmaphysik, Germany
Jolan Moldvai, Reports Library, Hungarian Academy of Sciences, Central Research Institute for Physics, Hungary
Dr. P. Kaw, Institute for Plasma Research, India
Ms. P.J. Pathak, Librarian, Institute for Plasma Research, India
Dr. Pandji Triadyaksa, Fakultas MIPA Universitas Diponegoro, Indonesia
Professor Sami Cuperman, Plasma Physics Group, Tel Aviv University, Israel
Ms. Clelia De Palo, Associazione EURATOM-ENEA, Italy
Dr. G. Grosso, Instituto di Fisica del Plasma, Italy
Librarian, Naka Fusion Research Establishment, JAERI, Japan
Library, Laboratory for Complex Energy Processes, Institute for Advanced Study, Kyoto University, Japan
Research Information Center, National Institute for Fusion Science, Japan
Professor Toshitaka Idehara, Director, Research Center for Development of Far-Infrared Region, Fukui University, Japan
Dr. O. Mitarai, Kyushu Tokai University, Japan
Mr. Adefila Olumide, Ilorin, Kwara State, Nigeria
Dr. Jiangang Li, Institute of Plasma Physics, Chinese Academy of Sciences, People's Republic of China
Professor Yuping Huo, School of Physical Science and Technology, People's Republic of China
Library, Academia Sinica, Institute of Plasma Physics, People's Republic of China
Librarian, Institute of Physics, Chinese Academy of Sciences, People's Republic of China
Dr. S. Mirnov, TRINITI, Troitsk, Russian Federation, Russia
Dr. V.S. Strelkov, Kurchatov Institute, Russian Federation, Russia
Kazi Firoz, UPJS, Kosice, Slovakia
Professor Peter Lukac, Katedra Fyziky Plazmy MFF UK, Mlynska dolina F-2, Komenskeho Univerzita, SK-842 15 Bratislava, Slovakia
Dr. G.S. Lee, Korea Basic Science Institute, South Korea
Dr. Rasulkhozha S. Sharafiddinov, Theoretical Physics Division, Insitute of Nuclear Physics, Uzbekistan
Institute for Plasma Research, University of Maryland, USA
Librarian, Fusion Energy Division, Oak Ridge National Laboratory, USA
Librarian, Institute of Fusion Studies, University of Texas, USA
Librarian, Magnetic Fusion Program, Lawrence Livermore National Laboratory, USA
Library, General Atomics, USA
Plasma Physics Group, Fusion Energy Research Program, University of California at San Diego, USA
Plasma Physics Library, Columbia University, USA
Alkesh Punjabi, Center for Fusion Research and Training, Hampton University, USA
Dr. W.M. Stacey, Fusion Research Center, Georgia Institute of Technology, USA
Director, Research Division, OFES, Washington, D.C. 20585-1290

The Princeton Plasma Physics Laboratory is operated
by Princeton University under contract
with the U.S. Department of Energy.

Information Services
Princeton Plasma Physics Laboratory
P.O. Box 451
Princeton, NJ 08543

Phone: 609-243-2750
Fax: 609-243-2751
e-mail: pppl_info@pppl.gov
Internet Address: http://www.pppl.gov